

Insights into the Thermal Fragmentation of Intramolecularly Coordinated Gallanes. A Matrix-Isolation FTIR Study

Eliza Gemel[†] and Jens Müller^{*‡}

Department of Chemistry, University of Saskatchewan, 110 Science Place, Saskatoon, Saskatchewan, S7N 5C9 Canada, and Lehrstuhl für Anorganische Chemie II, Organometallics and Materials Chemistry, Ruhr-Universität Bochum, 44780 Bochum, Germany

Received December 30, 2003

High-vacuum thermolyses (400–1000 °C) of the intramolecularly coordinated gallanes [Me₂N(CH₂)₃]₂GaX [X = Cl (**1**), Br (**2**)] and (Me₂NCH₂CD₂CH₂)₂GaBr (**2D**₄) have been investigated with matrix-isolation FTIR techniques. Around 850 °C, the fragmentation of these compounds was completed, and their typical IR absorptions could no longer be detected in argon matrices. Products have been identified with IR spectroscopy with the help of ab initio and DFT calculations and known literature data. In the case of precursors **1** and **2**, respectively, we identified GaH₃, XGaH₂, X₂GaH, GaH, GaX, HX, HCN, CH₄, H₂C=CH₂, H₂C=CHCH₃, H₂C=NMe, [H₂CCHCH₂]^{*}, and H₂C=CHCH₂NMe₂. In the case of the precursor **2D**₄, we found GaH₃, GaH₂D, BrGaH₂, BrGaDH, GaH, GaD, GaBr, HBr, HCN, CH₄, H₂C=CD₂, H₂C=CDCH₃, H₂C=NMe, [H₂CCDCH₂]^{*}, and H₂C=CDCH₂NMe₂. Among the monomeric hydrides, BrGaH₂ and BrGaDH were isolated for the first time. These compounds have been characterized by their six normal modes, and the experimental frequencies have been compared to the results of MP2(fc)/6-311+G(2d,p) and B3LYP/6-311+G(2d,p) calculations. These results have been interpreted by assuming that the intramolecularly coordinated precursors **1**, **2**, and **2D**₄ eliminate their ligands through Ga–C homolysis and β-hydrogen elimination.

Introduction

The interest in group 13 nitrides AlN, GaN, InN, and Al_x-Ga_yIn_zN as materials for various applications including light-emitting devices^{1–7} has prompted research groups to find single-source precursors (SSPs) for the chemical vapor deposition (CVD) of these materials. From a chemical point of view, azides might be ideal SSPs because the azido group acts as an intrinsic N source by elimination of N₂ as a harmless product.⁸ Among the known azides of the heavier group 13 elements, the intramolecularly coordinated precursors Me₂N(CH₂)₃Ga(N₃)₂⁹ and [Me₂N(CH₂)₃]₂MN₃ (M =

Al,^{10,11} Ga,¹² In^{13,14}) had been intensively used by R. A. Fischer et al. for nitride deposition.⁸ To date, detailed molecular fragmentation processes are unknown for the majority of CVD precursors. However, this lack of knowledge prevents a rational design of new precursors for improved material properties. Recently, in a series of matrix-isolation thermolysis experiments, we investigated the fragmentation of precursors of the type Me₂N(CH₂)₃GaX₂ (X = Cl, Br, Me, N₃).^{15–19} We have shown that the diazido gallane

* To whom correspondence should be addressed. E-mail: jens.mueller@usask.ca.

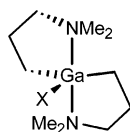
[†] Ruhr-Universität Bochum.

[‡] University of Saskatchewan.

- (1) Jones, A. C.; Whitehouse, C. R.; Roberts, J. S. *Chem. Vap. Deposition* **1995**, *1*, 65–74.
- (2) Akasaki, I.; Amano, H. *J. Cryst. Growth* **1995**, *146*, 455–461.
- (3) Neumayer, D. A.; Ekerdt, J. G. *Chem. Mater.* **1996**, *8*, 9–25.
- (4) Matsuoka, T. *Adv. Mater.* **1996**, *8*, 496–479.
- (5) Ponce, F. A.; Bour, D. P. *Nature* **1997**, *386*, 351–359.
- (6) Nakamura, S.; Fasol, G. *The Blue Laser Diode, GaN Based Light Emitters and Lasers*; Springer: Berlin, 1997.
- (7) Nakamura, S. *Science* **1998**, *281*, 951–961.
- (8) Müller, J. *Coord. Chem. Rev.* **2002**, *235*, 105–119.

- (9) Wohlfart, A.; Devi, A.; Maile, E.; Fischer, R. A. *Chem. Commun.* **2002**, 998–999.
- (10) Fischer, R. A.; Miehr, A.; Sussek, H.; Pritzkow, H.; Herdtweck, E.; Müller, J.; Ambacher, O.; Metzger, T. *Chem. Commun.* **1996**, 2685–2686.
- (11) Müller, J.; Fischer, R. A.; Sussek, H.; Pilgram, P.; Wang, R.; Pritzkow, H.; Herdtweck, E. *Organometallics* **1998**, *17*, 161–166.
- (12) Devi, A.; Sussek, H.; Pritzkow, H.; Winter, M.; Fischer, R. A. *Eur. J. Inorg. Chem.* **1999**, 2127–2134.
- (13) Fischer, R. A.; Miehr, A.; Metzger, T.; Born, E.; Ambacher, O.; Angerer, H.; Dimitrov, R. *Chem. Mater.* **1996**, *8*, 1356–1359.
- (14) Parala, H.; Devi, A.; Hipler, F.; Birkner, A.; Fischer, R. A. *Proc. Electrochem. Soc.* **2001**, *13*, 356–364.
- (15) Müller, J.; Sternkicker, H. *J. Chem. Soc., Dalton Trans.* **1999**, 4149–4153.
- (16) Müller, J.; Sternkicker, H.; Bergmann, U.; Atakan, B. *J. Phys. Chem. A* **2000**, *104*, 3627–3634.

Chart 1



does not fragment via β -hydrogen elimination and the detected thermolysis products could be explained by assuming a homolysis of the Ga–C bond in the initial stages of the process.¹⁸ Interestingly, we identified monomeric GaN₃ as a thermolysis product which might be a key intermediate of the nitride deposition with Me₂N(CH₂)₃Ga(N₃)₂.¹⁷

In the present paper we report on first insights into the fragmentation of organometallic gallanes that are equipped with two dimethylaminopropyl ligands. This might be a first step toward a better understanding of the pyrolysis behavior of azide SSPs of the general formula [Me₂N(CH₂)₃]₂MN₃ (M = Al, Ga, In) (Chart 1).

Experimental Section

General Remarks. All manipulations were performed under an inert atmosphere of purified argon using Schlenk techniques. The solvents were dried by standard procedures, distilled, and stored under argon and molecular sieves (4 Å). NMR spectra were obtained on a Bruker Advance DRX 400 (ambient temp; 400.13 and 100.62 MHz for ¹H and ¹³C, respectively) calibrated against residual protons of the deuterated solvents. ¹H and ¹³C chemical shifts are reported relative to TMS. Elemental analyses (C, H, N) were measured on a Carlo Erba EA 1110 CHN-O. MS data were obtained on a Varian MAT CH5 (70 eV). The reagents Li(CH₂)₃N(CH₃)₂,²⁰ LiCH₂CD₂CH₂NMe₂,¹⁹ and [Me₂N(CH₂)₃]₂GaCl (**1**)²¹ were prepared according to the literature procedures and analyzed by standard methods. Compound **1** (75–80 °C) and GaBr₃ (80–90 °C) were sublimed in a vacuum (10⁻²–10⁻³ mbar) prior to use.

[Me₂N(CH₂)₃]₂GaBr (2**).** To a solution of GaBr₃ (1.60 g, 5.17 mmol) in Et₂O (30 mL) and toluene (30 mL) Li(CH₂)₃NMe₂ (1.01 g, 10.85 mmol) was added at –78 °C (acetone/dry ice bath). Subsequently, the cooling bath was removed and the reaction mixture stirred for 12 h. All at ambient temperature, volatile components of the colorless clear solution were removed in a vacuum, toluene (20 mL) was added to the remaining solid, and the solution was separated by filtration from the colorless precipitate. Toluene was removed in a vacuum at ambient temperature to leave 1.80 g of a crude material behind. After two sublimations, analytically pure **2** was obtained (1.42 g, 4.41 mmol, 85%). ¹H NMR (400.13 MHz, C₆D₆): δ 0.62 (s, br, 4H, GaCH₂), 1.55 (s, br, 2H, GaCH₂CHH), 1.75 (s, br, 4H, GaCH₂CHH and NCHH), 1.96 (s, 12H, NCH₃), 2.47 (s, br, 2H, NCHH). ¹³C{¹H} (100.62 MHz, C₆D₆): δ 9.92 (GaCH₂), 22.36 (GaCH₂CH₂), 45.46 (NCH₃), 60.66 (NCH₂). MS (70 eV): m/z (%) = 322 (6) [M⁺], 241 (10) [M⁺ – Br], 236 (22) [M⁺ – (CH₂)₃N], 86 (26) (C₅H₁₂N⁺), 58 (100) [H₂CN(CH₃)₂⁺]. Anal. Calcd for C₁₀H₂₄N₂GaBr (321.94): H, 7.51; C, 37.31; N, 8.70. Found: H, 7.20; C, 36.91; N, 8.63.

[Me₂NCH₂CD₂CH₂]₂GaBr (2D₄**).** In accordance with the method described for **2**, compound **2D₄** was synthesized. GaBr₃ (1.16 g, 3.75 mmol) and LiCH₂CD₂CH₂NMe₂ (0.75 g, 8.06 mmol) gave analytically pure **2D₄** (0.86 g, 2.67 mmol, 71%). ¹H NMR (400.13 MHz, C₆D₆): δ 0.60 (s, br, 4H, GaCH₂), 1.74 (s, br, 2H, NCHH), 1.96 (s, 12H, NCH₃), 2.46 (s, br, 2H, NCHH). ¹³C{¹H} (100.62 MHz, C₆D₆): δ 9.60 (GaCH₂), 45.50 (NCH₃), 60.50 (NCH₂). MS (70 eV): m/z (%) = 326 (6) [M⁺], 245 (5) [M⁺ – Br], 238 (12) [M⁺ – H₂CCD₂CH₂N], 88 (20) [H₂CCD₂CH₂N⁺], 58 (100) [H₂CN(CH₃)₂⁺]. Anal. Calcd for C₁₀H₂₀D₄N₂GaBr (325.94): C, 36.85; N, 8.59. Found: C, 36.98; N, 8.81.

Matrix Isolation. The matrix apparatus consists of a vacuum line (Leybold Turbovac 151; Leybold Trivac D4B) and a Displex CSW 202 cryogenic closed-cycle system (ADP Cryogenics Inc.) fitted with CsI windows. Compounds were kept in a small heatable metal container connected to the matrix apparatus. In a typical experiment, the starting compound was connected to high vacuum at constant temperatures (57–70 °C for **1**; 75–85 °C for **2** and **2D₄**) while a flow of argon was conducted over the sample (Linde 6.0; 1.25 sccm). This gaseous mixture was passed through a thermolysis oven and deposited onto the CsI window at 15 K for 45–90 min. The oven was fitted with an Al₂O₃ tube with two parallel inner canals (outer diameter 4 mm; inner diameter 1 mm; the last 15 mm heated with tungsten wire); one of the inner canals was equipped with a thermocouple (Thermocoax: NiCrSi/NiSi), and the second one was used for the argon/precursor mixture. The hot end of the pyrolysis tube was 25 mm away from the cooled CsI window to ensure that maximum amounts of volatile fragments emerging from the oven were trapped in matrices. To ensure that the results are reproducible, we performed four extensive series of thermolysis experiments; first series with **1**, second with **2**, third with **2D₄**, followed by a last series with precursor **2** again.

After a deposition onto a CsI window at 15 K, the respective matrix was cooled to 10–11 K for IR measurements. IR spectra of the matrices were recorded on a Bruker EQUINOX 55 in the range 4000–200 cm⁻¹ with a resolution of 0.5 and 1.0 cm⁻¹ (KBr beam splitter for 4000–400 cm⁻¹ and Mylar beam splitter for the far-IR region from 700 to 200 cm⁻¹).

Measured IR frequencies of matrix-isolated species are indicated as follows: ○×○, BrGaH₂ (see Table 1); ○×●, BrGaDH (see Table 2); ○×○, ClGaH₂ (1978.3, 1965.4 cm⁻¹); ×○×, Br₂-GaH (1991.7, 596.7, 445.3 cm⁻¹); ○○○, GaH₃ (1923.0, 758.5, 717.3 cm⁻¹); ○●○, GaDH₂ (1923.3, 1921.1, 1385.6, 756.8, 660.5, 626.1 cm⁻¹); ○, GaH (1514.0 cm⁻¹); ●, GaD, 1090.6 cm⁻¹; a, H₂C=NCH₃ (1659.1, 1469.5, 1440.3, 1220.6, 1026.3, 478.4 cm⁻¹); b, H₂C=CH₂ (1440.3, 947.4 cm⁻¹); b', CH₂=CD₂ (945.8, 749.9 cm⁻¹); c, CH₄ (1305.7 cm⁻¹); d, [H₂CCHCH₂]^{*} (1388.7, 983.5, 801.1 cm⁻¹); d', [H₂CCDCH₂]^{*} (803.0, 786.6 cm⁻¹); e, H₂C=CHCH₃ (998.0, 908.6, 578.3 cm⁻¹; tentative assignment, see text); e', H₂C=CDCH₃ (908.6 cm⁻¹; tentative assignment, see text); f, H₂C=CHCH₂NMe₂ (1417.4, 1350.1, 1266.8, 1181.4, 1173.2, 1096.4, 1043.7, 1038.4, 1000.5, 963.2, 922.6, 920.2, 918.0, 854.9, 850.0 cm⁻¹); f', H₂C=CDCH₂NMe₂ (1349.7, 1181.4, 1096.2, 1043.7, 1038.4, 1033.4, 922.7, 919.8 cm⁻¹); g, HCN (3306.0, 720.8 cm⁻¹); X, Me₂N(CH₂)₃GaBrH (max at 1902.2 cm⁻¹); XD, Me₂NCH₂CD₂CH₂GaBrH (max at 1902.2 cm⁻¹); Y, Me₂N(CH₂)₃GaClH (max at 1904.1 cm⁻¹).

Theoretical Calculations. All calculations have been carried out using the GAUSSIAN 98 program package.²² All geometry optimizations have been performed without geometrical constraints. As a hybrid HF-DFT method, the three-parameter exchange functional of Becke²³ with the correlation functional by Lee, Yang, and Parr²⁴ has been used (B3LYP). All MP2 calculations have

(17) Müller, J.; Bendix, S. *Chem. Commun.* **2001**, 911–912.

(18) Müller, J.; Wittig, B.; Sternkicker, H.; Bendix, S. *J. Phys. IV* **2001**, *11*, 17–22.

(19) Müller, J.; Wittig, B.; Bendix, S. *J. Phys. Chem. A* **2001**, *105*, 2112–2116.

(20) Thiele, K.-H.; Langguth, E.; Müller, G. E. *Z. Anorg. Allg. Chem.* **1980**, *462*, 152–158.

(21) Schumann, H.; Seuss, T. D.; Just, O.; Weimann, R.; Hemling, H.; Görlitz, F. H. *J. Organomet. Chem.* **1994**, *479*, 171–186.

Table 1. Observed IR Frequencies and Calculated Harmonic Frequencies of ClGaH₂ and BrGaH₂

		exptl freq ^a [cm ⁻¹]	MP2(fc)/6-311+G(2d,p)		obsd/calcd freq ratio	B3LYP/6-311+G(2d,p)		obsd/calcd freq ratio	
			freq ^a [cm ⁻¹]	int [km mol ⁻¹]		freq ^a [cm ⁻¹]	int [km mol ⁻¹]		
ClGaH ₂									
A ₁	ν ₁	ν _s (GaH ₂)	1964.9	2060.2	75.8	0.9537	2026.4	59.6	0.9697
	ν ₂	δ(GaH ₂)	731.4	751.1	212.4	0.9738	725.7	155.9	1.0079
	ν ₃	ν(GaCl)	407.2	421.5	79.0	0.9661	399.8	69.4	1.0185
B ₁	ν ₄	ν _{as} (GaH ₂)	1978.2	2065.4	213.7	0.9578	2043.2	192.9	0.9682
	ν ₅	δ(HGaCl)	510.0	499.4	47.2	1.0212	495.2	35.9	1.0299
B ₂	ν ₆	γ(H)	619.9	624.4	134.2	0.9928	620.0	87.0	0.9998
BrGaH ₂									
A ₁	ν ₁	ν _s (GaH ₂)	1958.3	2056.7	93.7	0.9521	2021.2	72.6	0.9689
	ν ₂	δ(GaH ₂)	725.5	750.7	252.2	0.9664	722.5	201.0	1.0042
	ν ₃	ν(GaBr) ^b	297.7	302.6	40.8	0.9838	291.6	37.4	1.0209
B ₁	ν ₄	ν _{as} (GaH ₂)	1973.2	2063.3	205.8	0.9563	2039.7	186.3	0.9674
	ν ₅	δ(HGaBr)	494.8	489.0	32.9	1.0119	479.6	24.3	1.0317
B ₂	ν ₆	γ(H)	609.6	616.0	116.7	0.9896	604.7	75.4	1.0081

^aListed are wavenumbers concerning the main isotopomer. ^bν(GaBr) shows an isotopic pattern (see Figure 2).

Table 2. Observed IR Frequencies and Calculated Harmonic Frequencies of BrGaDH

		exptl freq [cm ⁻¹]	MP2(fc)/6-311+G(2d,p)		obsd/calcd freq ratio	B3LYP/6-311+G(2d,p)		obsd/calcd freq ratio	
			freq [cm ⁻¹]	int [km mol ⁻¹]		freq [cm ⁻¹]	int [km mol ⁻¹]		
BrGaDH									
A'	ν ₁	ν _s (GaH)	1966.7	2059.8	153.6	0.9548	2030.3	133.6	0.9687
	ν ₂	δ(GaHD)	654.1	673.7	191.9	0.9709	649.5	152.1	1.0071
	ν ₃	ν(GaBr)	297.6	302.1	39.1	0.9851	291.2	36.0	1.0220
	ν ₄	ν(GaD)	1415.1	1467.4	76.1	0.9644	1446.3	64.8	0.9784
	ν ₅	δ(HGaBr)	393.9	391.4	28.2	1.0064	382.8	21.7	1.0290
A''	ν ₆	γ(HD)	534.7	537.8	89.9	0.9942	528.0	58.2	1.0127

been performed with the frozen core (fc) approximation. Analysis of the vibrational frequencies at all applied levels of theory confirmed that respective molecules correspond to local minima at a potential energy surface. The absolute energies in Hartrees and zero point vibrational energies, ZPVE, in kJ/mol (values in parentheses) are as follows: ClGaH₂, -2386.336575 (37.74) [B3LYP/6-311+G(2d,p)], -2383.924573 (38.41) [MP2(fc)/6-311+G(2d,p)]; BrGaH₂, -4500.253451 (36.84) [B3LYP/6-311+G(2d,p)], -4496.781171 (37.55) [MP2(fc)/6-311+G(2d,p)]; Me₂N(CH₂)₃GaHCl, isomer A/isomer B (Figure 6), -2632.150653 (500.96)/-2632.149958 (501.15) [HF/6-31G(d)], -2636.321693 (469.33)/-2636.320868 (469.36) [B3LYP/6-31G(d)], -2638.346768 (463.93), -2638.346042 (463.62) [B3LYP/6-311G(d,p)]; Me₂N(CH₂)₃GaHBr, isomer A/isomer B (Figure 6), -4742.572371 (500.35)/-4742.571812 (500.66) [HF/6-31G(d)], -4747.842113 (469.08)/-4747.841438 (468.91) [B3LYP/6-31G(d)], -4752.268753 (463.02), -4752.268071 (462.97) [B3LYP/6-311G(d,p)].

The B3LYP/6-311+G(2d,p) harmonic frequencies [cm⁻¹] for BrGaD₂ are as follows (intensities [km/mol] in parentheses): 1455.2 (98.6), 1432.8 (40.0), 514.6 (107.5), 437.8 (41.0), 346.6 (13.5), 290.9 (35.8).

(22) Frisch, M. J.; Trucks, G. W.; Schlegel, H. B.; Scuseria, G. E.; Robb, M. A.; Cheeseman, J. R.; Zakrzewski, V. G.; Montgomery, J. A., Jr.; Stratmann, R. E.; Burant, J. C.; Dapprich, S.; Millam, J. M.; Daniels, A. D.; Kudin, K. N.; Strain, M. C.; Farkas, O.; Tomasi, J.; Barone, V.; Cossi, M.; Cammi, R.; Mennucci, B.; Pomelli, C.; Adamo, C.; Clifford, S.; Ochterski, J.; Petersson, G. A.; Ayala, P. Y.; Cui, Q.; Morokuma, K.; Malick, D. K.; Rabuck, A. D.; Raghavachari, K.; Foresman, J. B.; Cioslowski, J.; Ortiz, J. V.; Stefanov, B. B.; Liu, G.; Liashenko, A.; Piskorz, P.; Komaromi, I.; Gomperts, R.; Martin, R. L.; Fox, D. J.; Keith, T.; Al-Laham, M. A.; Peng, C. Y.; Nanayakkara, A.; Gonzalez, C.; Challacombe, M.; Gill, P. M. W.; Johnson, B. G.; Chen, W.; Wong, M. W.; Andres, J. L.; Head-Gordon, M.; Replogle, E. S.; Pople, J. A. *Gaussian 98*, revision A.11; Gaussian, Inc.: Pittsburgh, PA, 1998.

(23) Becke, A. D. *J. Chem. Phys.* **1993**, *98*, 5648–5652.

(24) Lee, C.; Yang, W.; Parr, R. G. *Phys. Rev. B* **1988**, *37*, 785–789.

The B3LYP/6-311+G(2d,p) harmonic frequencies [cm⁻¹] for XGaH[•] are as follows (intensities [km/mol] in parentheses): ClGaH[•] 1675.5 (129.9), 509.9 (35.2), 373.4 (64.4); BrGaH[•] 1676.0 (135.8), 497.1 (31.6), 269.2 (35.3).

The isotopic pattern of Figure 2 was calculated on the B3LYP/6-311+G(2d,p) level with the assumption of a Gauss line shape profile. The calculated unscaled harmonic frequencies (cm⁻¹) and intensities (km/mol; in parentheses) for ν₃ for the four main isotopomers with natural abundances in percent are the following: 30.5% H₂⁶⁹Ga⁷⁹Br 291.57 (37.4), 29.9% H₂⁶⁹Ga⁸¹Br 289.87 (36.9), 20.0% H₂⁷¹Ga⁷⁹Br 289.41 (36.9), 19.6% H₂⁷¹Ga⁸¹Br 287.69 (36.4).

Results and Discussion

Thermolysis of [Me₂N(CH₂)₃]₂GaX [X = Cl (1**) and X = Br (**2**)].** We carried out a series of high-vacuum thermolyses in the temperature range 400–1000 °C of compounds **1** and **2**, respectively. Around 850 °C, the fragmentations of the starting compounds were completed, and their typical IR absorptions could no longer be detected in argon matrices.

Figure 1 shows a representative IR spectrum of the intermediates of a thermolysis of **2** at 850 °C trapped in argon at 15 K (Figure 1, spectrum A). The most informative area of this rich spectrum is the gallium hydrogen stretching region at the high-frequency end of spectrum A. In this range, four sharp and intense bands at 1991.7, 1973.2, 1958.3, and 1923.0 cm⁻¹ are present. The smallest one at 1991.7 cm⁻¹ is certainly caused by Br₂GaH, which exhibits two other IR bands at 596.7 cm⁻¹ [δ(BrGaH)] and at 445.5 cm⁻¹ [γ(H)] in the depicted spectrum A (indication ×○×).¹⁵ The IR band at 1923.0 cm⁻¹ can be assigned to the degenerated Ga–H stretching modes of monomeric GaH₃. Moreover, our measured IR bands at 758.5 cm⁻¹ [δ_{as}(GaH₂)] and 717.3

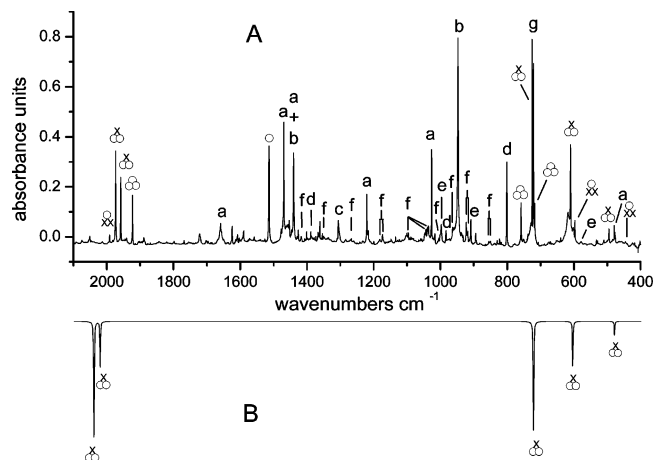


Figure 1. Spectrum A shows the matrix-isolated products of a thermolysis of **2** at 850 °C trapped in an excess of argon at 15 K (see Experimental Section for details): $\circ \times \circ$, BrGaH_2 ; $\times \circ \times$, Br_2GaH ; $\circ \circ \circ$, GaH_3 ; \circ , GaH ; a, $\text{H}_2\text{C}=\text{NCH}_3$; b, $\text{H}_2\text{C}=\text{CH}_2$; c, CH_4 ; d, $[\text{H}_2\text{CCHCH}_2]^+$; e, $\text{H}_2\text{C}=\text{CHCH}_3$; f, $\text{H}_2\text{C}=\text{CHCH}_2\text{NMe}_2$; g, HCN . Spectrum B is the calculated IR spectrum of BrGaH_2 ($\circ \times \circ$) at the B3LYP/6-311+G(2d,p) level (Table 1).

cm^{-1} [$\gamma(\text{H})$] match with the published data of this well-known molecule (published values are 1923.2, 758.7, and 717.4 cm^{-1} ; Figure 1 indication $\circ \circ \circ$).²⁵ We assigned two remaining IR bands at 1973.2 and 1958.3 cm^{-1} to the antisymmetric and symmetric Ga–H stretching modes of monomeric BrGaH_2 , respectively. In the case of the chloride compound **1**, the Ga–H stretching modes absorb at 1978.2 and 1964.9 cm^{-1} . Even without any calculations, there is no doubt that monomeric ClGaH_2 was formed in the pyrolysis of the gallane **1**, because ClGaH_2 was photochemically synthesized in argon matrices and had been characterized by IR spectroscopy, ab initio calculations, and normal coordinate analysis.²⁶ Within the experimental error, our measured frequencies as well as intensities of ClGaH_2 match with the published data.

Table 1 shows the experimental and calculated IR data of ClGaH_2 and BrGaH_2 . For the assignment of harmonic frequencies we have chosen the MP2 and B3LYP method with a 6-311+G(2d,p) basis set. The C_{2v} symmetrical gallanes ClGaH_2 and BrGaH_2 are expected to show six normal modes belonging to the irreducible representations $A_1(3)$, $B_1(2)$, and $B_2(1)$. We assigned all six normal modes to measured IR bands for ClGaH_2 and for the hitherto unknown BrGaH_2 . A calculated IR spectrum of BrGaH_2 is depicted in Figure 1 to illustrate the assignment and the fit between theory and experiment. This fit is also demonstrated in Table 1 by observed/calculated frequency ratios which were found in the ranges 0.9521–1.0212 (ClGaH_2) and 0.9522–1.0119 (BrGaH_2) at the MP2 level and in the ranges 0.9682–1.0299 (ClGaH_2) and 0.9674–1.0317 (BrGaH_2) at the B3LYP level of theory (Table 1).

As expected, similar frequency ratios are observed for similar normal modes of ClGaH_2 in comparison with BrGaH_2 on both levels of theory. This strongly supports the correct-

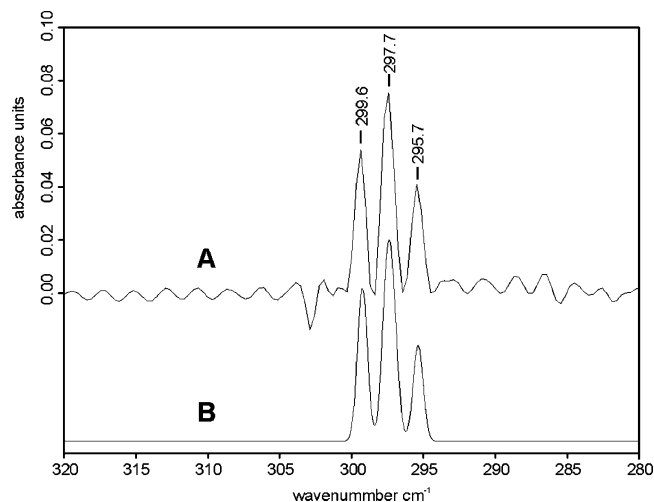


Figure 2. Observed (spectrum A) and calculated (spectrum B) isotopic pattern of ν_3 of BrGaH_2 (scaling factor of 1.021; see Experimental Section, last paragraph for details).

ness of the assignment for the hitherto unknown bromogallane BrGaH_2 . Additional support comes from a distinct isotopic pattern for the Ga–Br stretch ν_3 which is caused by two gallium and two bromine isotopes. Only this mode is expected to give a detectable natural isotopic pattern within our spectral resolution. Figure 2 compares the measured IR band (spectrum A) with the predicted isotopic pattern. Even though the intensity of this IR band is quite low, the exact match of the detected and measured isotopic pattern shown in Figure 2 proves the assignment to be correct.

One of the most intense IR bands in Figure 1 appears at 1514.0 cm^{-1} (indication \circ). This absorption is present in all measured thermolysis matrix spectra of **1** and **2**, respectively. Its relative intensity with respect to IR bands of other molecules varies at different thermolysis temperatures, and we could not identify other IR bands that showed the same behavior. Furthermore, the small half-band-width of this IR band hints to a small molecule. The reported stretching frequency of monomeric GaH that was matrix isolated in Ar (1514.1 cm^{-1} ,²⁷ 1513.8 cm^{-1} ²⁸) matches with our value, and consequently, we assign the IR band at 1514.0 cm^{-1} to GaH .

In addition to gallium hydrides discussed so far, we have identified organic and inorganic species resulting from the decomposition of **1** and **2**, respectively. These assignments are based on known literature data including our experience with fragmentations of compounds equipped with the dimethylaminopropyl ligand. As it is indicated in Figure 1, we identified $\text{H}_2\text{C}=\text{NCH}_3$,^{29,30} CH_4 ,³¹ $\text{H}_2\text{C}=\text{CH}_2$,³² $\text{H}_2\text{C}=\text{CHCH}_3$,³³ $[\text{H}_2\text{CCHCH}_2]^+$,³⁴ HCN ,^{35,36} and $\text{Me}_2\text{NCH}_2\text{CH}=\text{CH}_2$.¹⁶ Furthermore, GaX ($X = \text{Cl}$,³⁷ Br ¹⁵) and HX ($X = \text{Cl}$, Br)^{38–40} are among the thermolysis products, but their typical IR bands are out of the range of spectrum A.

A comment is needed on the identification of propene, $\text{H}_2\text{C}=\text{CHCH}_3$ (see Figure 1, indication e). We found three IR bands at 998.0, 908.6, and 578.3 cm^{-1} that match well

(25) Pullumbi, P.; Bouteiller, Y.; Manceron, L.; Mijoule, C. *Chem. Phys.* **1994**, *185*, 25–37.

(26) Köppe, R.; Schnöckel, H. *J. Chem. Soc., Dalton Trans.* **1992**, 3393–3395.

(27) Xiao, Z. L.; Hauge, R. H.; Margrave, J. L. *Inorg. Chem.* **1993**, *32*, 642–646.

(28) Pullumbi, P.; Mijoule, C.; Manceron, L.; Bouteiller, Y. *Chem. Phys.* **1994**, *185*, 13–24.

with published values of 997.8, 909.9, and 578.6 cm^{-1} ³³ for this species. However, the IR band at 998.0 cm^{-1} is indistinguishable from an IR absorption of allyldimethylamine, and the IR band at 578.3 cm^{-1} is very weak (Figure 1). The most intense and, hence, the most indicative IR band is the one at 908.6 cm^{-1} that would correspond to a CH_2 wagging mode of propene. According to recent calculations⁴¹ the next most intense modes for propene are CH stretches, but the CH stretching region of the thermolysis experiments with **2** is highly populated by IR bands and an assignment would be uncertain. That means that the identification of propene is based on a tentative assignment of only two IR bands.

Thermolysis of $(\text{Me}_2\text{NCH}_2\text{CD}_2\text{CH}_2)_2\text{GaBr}$ (2D₄**).** For a deeper insight into the fragmentation processes, we performed thermolysis studies with the deuterated gallane $(\text{Me}_2\text{NCH}_2\text{CD}_2\text{CH}_2)_2\text{GaBr}$ (**2D₄**). By using the selectively deuterated donor ligand $\text{Me}_2\text{NCH}_2\text{CD}_2\text{CH}_2$, one can experimentally determine if β -hydrogen elimination occurs. In a former study, we were able to show that the dimethylgallane $\text{Me}_2\text{NCH}_2\text{CD}_2\text{CH}_2\text{GaMe}_2$ fragments mainly via a β -hydrogen elimination path resulting in monomeric DGaMe_2 .¹⁹ As in the case of the nondeuterated compound **2**, we performed a series of high-vacuum thermolyses with compound **2D₄** in the temperature range 400–1000 °C.

Gallium Hydrides and Deuterides. The results of a thermolysis of **2D₄** at 850 °C are illustrated in Figures 3 and 4. Figure 3 depicts the typical IR range for Ga–H stretches and compares the results of **2D₄** with those of the nondeuterated precursor **2**.

From a first glance at the IR spectra of Figure 3, it is obvious that the most intense IR bands of the thermolysis of **2D₄** are due to the formation of BrGaH_2 (Figure 3A, indication $\text{O}\times\text{O}$). However, a new IR band at 1966.7 cm^{-1} appears right in the middle of the two IR bands of BrGaH_2 (Figure 3A, indication $\text{O}\times\bullet$). The frequency and the fact that it is only a single IR band in the typical Ga–H stretching region can be interpreted as being caused by the monodeuterated species BrGaDH . The differences between two frequencies of the asymmetric and symmetric Ga–H modes of BrGaH_2 are due to the interaction of the two H atoms.

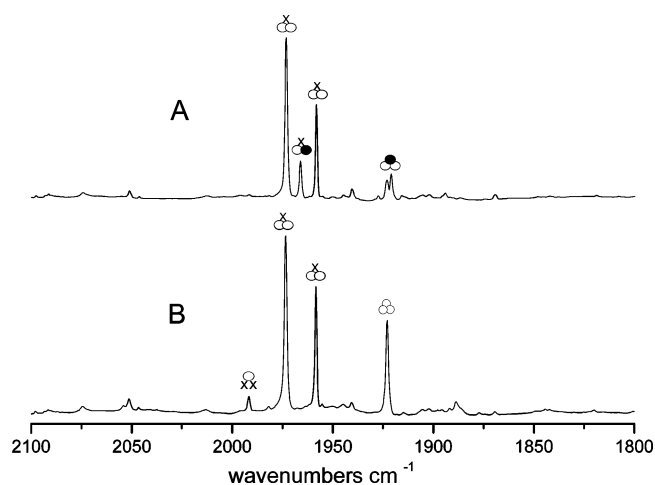


Figure 3. Experimental IR spectra of products of the thermolysis **2D₄** (spectrum A) and **2** (spectrum B) at 850 °C, respectively, trapped in an excess of argon at 15 K. Spectrum A: $\text{O}\times\text{O}$, BrGaH_2 ; $\text{O}\times\bullet$, BrGaDH ; $\text{O}\bullet\text{O}$, GaDH_2 . Spectrum B: xOx , Br_2GaH ; $\text{O}\times\text{O}$, BrGaH_2 ; OOO , GaH_3 .

This interaction is negligible for BrGaDH caused by a large difference between atomic masses of H and D. Consequently, BrGaDH is expected to show an “undisturbed” Ga–H stretching motion. We have assigned all six fundamental vibrations of BrGaDH to measured IR bands for this C_s symmetrical molecule ($5 \times A'$ and $1 \times A''$). Figure 4 shows an IR spectrum of matrix-isolated species from the thermolysis of **2D₄** with $\text{O}\times\bullet$ indicating the assignment for BrGaDH . All experimental and calculated vibrational data of BrGaDH are compiled in Table 2.

As expected, similar vibrational modes of the two isotopomers BrGaH_2 and BrGaDH lead to similar obsd/calcd frequency ratios (Tables 1 and 2). One particular interesting mode is the Ga–D stretching mode which gives an experimental isotopic shift of 1.390 if we compare the $\nu(\text{GaH})$ with the $\nu(\text{GaD})$ of BrGaDH . The calculated value of 1.404 on both levels of theory is slightly higher than the measured one. A similar difference between predicted and measured isotopic shifts was determined for the two isotopomers Me_2GaH and Me_2GaD : isotopic shifts of 1.387 (exptl) and of 1.404 [MP2(fc)/6-311+G(2d,p) level].¹⁵

The identification of BrGaH_2 and BrGaDH in the thermolysis experiments with the selectively deuterated compound **2D₄** raises the question if BrGaD_2 is among the thermolysis products. On the basis of the predicted vibrational spectrum of BrGaD_2 , we could not find experimental hints for this species (see Experimental Section, last paragraph, for details). Therefore, we assume that if the compound is among the thermolysis products, the amount is negligible low in comparison with BrGaDH .

Additional differences between the thermolysis experiments with **2D₄** and **2** can be seen in Figure 3. Fragmentation of **2** results in one intense IR band at 1923.0 cm^{-1} (GaH_3) whereas **2D₄** results in a “doublet” at 1923.5 and 1921.2 cm^{-1} . These facts point to gallane with a reduced symmetry, and they hint to GaDH_2 (C_{2v} symmetry). Fortunately, the complete set of possible deuterides of the parent gallane GaDH_2 , GaD_2H , and GaD_3 are known in argon matrices.²⁵ The published vibrational frequencies and intensities of

- (29) Hinze, J.; Curl, R. F., Jr. *J. Am. Chem. Soc.* **1964**, *86*, 5068–5070.
 (30) Stolklin, I.; Ha, T.-K.; Günthard, H. H. *Chem. Phys.* **1977**, *21*, 327–347.
 (31) Huang, J. W.; Graham, W. R. M. *J. Chem. Phys.* **1990**, *93*, 1583–1596.
 (32) Andrews, L.; Johnson, G. L.; Kelsall, B. J. *J. Chem. Phys.* **1982**, *76*, 5767–5773.
 (33) Andrews, L.; Johnson, G. L.; Kelsall, B. J. *J. Am. Chem. Soc.* **1982**, *104*, 6180–6186.
 (34) Nandi, S.; Arnold, P. A.; Carpenter, B. K.; Nimlos, M. R.; Dayton, D. C.; Ellison, G. B. *J. Phys. Chem. A* **2001**, *105*, 7514–7524.
 (35) Milligan, D. E.; Jacox, M. E. *J. Chem. Phys.* **1963**, *39*, 712–715.
 (36) Lanzisera, D. V.; Andrews, L. *J. Phys. Chem. A* **1997**, *101*, 824–830.
 (37) Samsonova, E. D.; Osin, S. B.; Shevel'kov, V. F. *Russ. J. Inorg. Chem.* **1988**, *33*, 1598.
 (38) Bowers, M. T.; Flygare, W. H. *J. Chem. Phys.* **1966**, *44*, 1389–1404.
 (39) Barnes, A. J.; Hallam, H. E.; Scrimshaw, G. F. *Trans. Faraday Soc.* **1969**, *65*, 3150–3158.
 (40) our measured values are 2888.2, 2785.7, and 2701.6 cm^{-1} for (HCl); 2569.0, 2452.1, and 2431.9 cm^{-1} for (HBr).
 (41) Radziszewski, J. G.; Downing, J. W.; Gudipati, M. S.; Balaji, V.; Thulstrup, E. W.; Michl, J. *J. Am. Chem. Soc.* **1996**, *118*, 10275–10284.

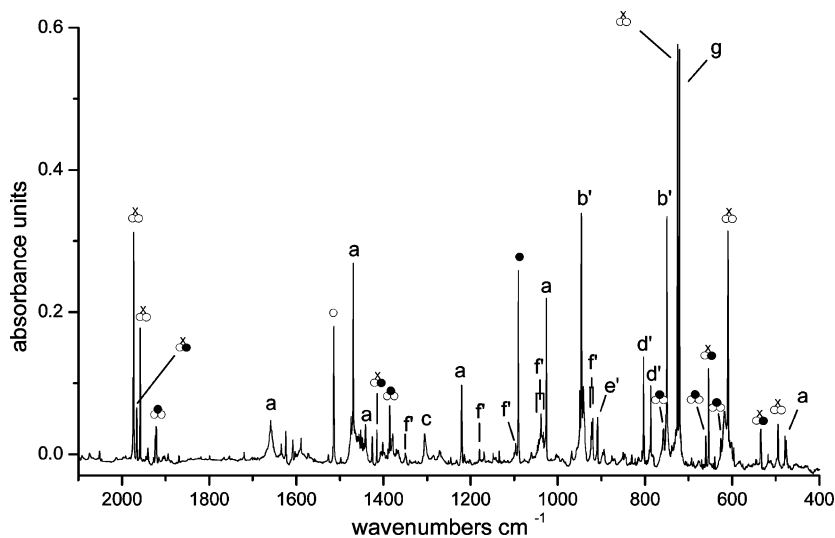


Figure 4. Products of a thermolysis of $2D_4$ at 850 °C trapped in an excess of argon at 15 K (see Experimental Section for details): $\circ \times \circ$, BrGaH₂; \circ , GaH; $\circ \times \bullet$, BrGaDH; \bullet , GaD; $\circ \bullet \circ$, GaDH₂; a, H₂C=NCH₃; b', CH₂=CD₂; c, CH₄; d', [H₂CCDCH₂]^{*}; e', H₂C=CDCH₃; f', H₂C=CDCH₂NMe₂; g, HCN.

GaDH₂ (1924.0, 1921.3, 1385.4, 756.9, 660.6, and 626.3 cm⁻¹) match very well with our assignments for GaDH₂ (1923.5, 1921.2, 1385.6, 756.8, 660.6, and 626.1 cm⁻¹) (Figures 3 and 4; indication $\circ \bullet \circ$). Very weak IR bands at 758.5 and 717.4 cm⁻¹ indicate the presence of small amounts of GaH₃. However, the absorption of $\nu(\text{GaH})$ of GaH₃ is obscured by the IR band at 1923.5 cm⁻¹ assigned to GaDH₂.

As in the case of the thermolysis of compound **2**, the fragmentation of the deuterated precursor $2D_4$ results in the formation of GaH (Figure 4, indication \circ). Furthermore, for all thermolysis experiments an intense IR band at 1090.6 cm⁻¹ appears in the IR spectra. We assign the intense band at 1090.6 cm⁻¹ to GaD. Our detected frequency matches very well with the published value for GaD (1090.3 cm⁻¹²⁷). Interestingly, the IR band of GaD is more intense than the one of GaH (Figure 4; indications \bullet and \circ). The relative amounts of GaD/GaH would be ca. 2.8:1.0 (Figure 4; peak heights have been taken as a measure of intensity), if one takes the calculated transition moments of 426 km/mol for GaD (1113.5 cm⁻¹) and 839 km/mol for GaH (1562.9 cm⁻¹) into account (B3LYP/6-311+G(2d,p) level²²). However, the GaD/GaH ratio depends on the applied thermolysis temperature: with increasing temperature the relative amount of GaD strongly decreases.⁴² So far, this reproducible effect is not understood.

Carbon-Containing Species and Further Products. The identification of products resulting from fragmentation of the chelating ligands gives important mechanistic insights into the thermolysis process. A comparison between the spectra resulting from compound **2** with those from $2D_4$ directly shows similarities and dissimilarities. Fragmentation of $2D_4$ resulted in CH₄, HCN, and H₂C=NCH₃, but H₂C=CH₂, [H₂CCHCH₂]^{*}, and Me₂NCH₂CH=CH₂ could not be detected. On the other hand, new IR bands in the thermolysis spectra

of $2D_4$ can be traced back to deuterated organic molecules. The two most intense new IR absorptions were found at 945.8 and 749.9 cm⁻¹ and match well with the published values of H₂C=CD₂ (945 and 749 cm⁻¹).³² A thorough study of the matrix-isolated allyl radicals [H₂CCHCH₂]^{*}, [H₂CCDCH₂]^{*}, and [D₂CCDCH₂]^{*} with polarized IR absorption spectroscopy have been published recently.³⁴ This paper also provides an overview of the previous investigations of allyl radicals. The published value of the most intense IR band of [H₂CCHCH₂]^{*} is 801 cm⁻¹ [$\nu(\text{CH}_2)_{\text{wag}}$] followed by the second intense mode at 983 cm⁻¹ [$\nu(\text{CH})_{\text{oop}}$].³⁴ As mentioned before, these data are in excellent agreement with the IR bands at 801.1 and 983.6 cm⁻¹ that we assigned to [H₂CCHCH₂]^{*} in the thermolysis experiments of precursor **2**; these IR bands are absent in the case of the precursor $2D_4$. Instead, two absorptions at 803.0 and 786.6 cm⁻¹ appear in this region (Figure 4, indication d'). We assign the IR band at 803.0 cm⁻¹ to $\nu(\text{CH}_2)_{\text{wag}}$ and the lower frequency mode to the $\nu(\text{CD})_{\text{oop}}$ of [H₂CCDCH₂]^{*}. These assignments are based on the published data for this monodeuterated species: the two most intense IR bands of this compound were detected at 802 and 787 cm⁻¹ with relative intensities of 1.00:0.71.³⁴

In a former thermolysis matrix-isolation study, we have shown that Me₂NCH₂CD₂CH₂GaMe₂ fragments to give monomeric DGaMe₂ and H₂C=CDCH₂NMe₂. The monodeuterated allyldimethylamine is a relatively weak IR absorber, but because Me₂NCH₂CD₂CH₂GaMe₂ mainly fragments via β -hydrogen elimination, we could clearly identify the most intense IR bands of this species, i.e., two bands at 2819.8 and 2779.6 cm⁻¹, a "triplet" at 1043.7, 1038.4, and 1033.4 cm⁻¹, and a "doublet" at 922.7 and 919.8 cm⁻¹. In thermolysis experiments with $2D_4$, the CH stretching region and the area around 1040 cm⁻¹ are very populated with IR bands, and an assignment of IR bands to H₂C=CDCH₂NMe₂ is possible but uncertain. However, a "doublet" at 922.8 and 919.7 cm⁻¹ gives a clear hint to the presence of the monodeuterated amine (Figure 4, indication f').

(42) In a continuous series of experiments, the following IR values were measured in absorbance units: 0.099 (GaD):0.078 (GaH) at 850 °C, 0.044 (GaD):0.068 (GaH) at 900 °C, and 0.024 (GaD):0.045 (GaH) at 1000 °C.

As mentioned before, we tentatively assigned three IR bands at 998.0, 908.6, and 578.3 cm^{-1} in the thermolysis experiments of **2** to $\text{H}_2\text{C}=\text{CHCH}_3$ (Figure 1, indication e). In the thermolysis experiments with **2D₄**, a weak IR band was again detected at 908.6 cm^{-1} . The value and the shape of this IR band matches exactly with the one that we assigned in experiments with **2** to $\text{H}_2\text{C}=\text{CHCH}_3$. From a chemical point of view, the monodeuterated propene $\text{H}_2\text{C}=\text{CDCH}_3$ is expected as a pyrolysis product of **2D₄**. To the best of our knowledge, an IR spectrum of matrix-isolated $\text{H}_2\text{C}=\text{CDCH}_3$ is not available in the literature. However, in the course of an investigation of transition moment directions, the IR spectra of propene and some of its isotopomers had been determined in stretched polyethylene at 12 K.⁴¹ Both isotopomers, $\text{H}_2\text{C}=\text{CHCH}_3$ and $\text{H}_2\text{C}=\text{CDCH}_3$, exhibit their most intense IR band at 908 cm^{-1} . This is in accordance with CCSD/6-311G(d,p) calculations that were discussed in the same publication.⁴¹ Against this background, it is possible that the IR band at 908.6 cm^{-1} in the spectrum of Figure 4 is due to the presence of $\text{H}_2\text{C}=\text{CDCH}_3$, but this only a tentative assignment.

In addition to the thermolysis products discussed so far, we could identify $(\text{HBr})_x$ (2569.0, 2452.1, 2431.9 cm^{-1})^{38,39} and GaBr (299.6, 297.7, 295.7 cm^{-1})¹⁵ by comparison with their known IR frequencies. On the basis of published data of $(\text{DBr})_x$, we could not find any IR absorptions for this species.³⁸ Keeping in mind that the IR transition moment is reduced by ca. 50% from HX to DX , it might be the case that $(\text{DBr})_x$ is present but its IR absorptions are below our detection limit.

Lower Thermolysis Temperature Range. We have discussed results of thermolyses at 850 °C of the precursors **1**, **2**, and **2D₄**, respectively. Under these conditions, a complete fragmentation occurs. However, around 600 °C new IR bands in the thermolysis spectra already indicate a beginning fragmentation.

Figure 5 shows the Ga–H stretching region of three representative spectra obtained from thermolysis experiments of precursors **1**, **2**, and **2D₄**, respectively. First, for all different precursors a broad but well-structured IR band around 1900 cm^{-1} is present. The intensity of this structured IR band increases from 600 to ca. 750 °C, it decreases at higher temperatures, and it is not detectable any longer at 850 °C. The compounds that are causing these IR resonances are obvious intermediates in the fragmentation process. If one compares the chloride **1** with the bromide **2** (Figure 5A,B), the structure of the IR bands around 1900 wavenumbers are comparable; only the frequencies are slightly different. For **1** the most intense IR band appears at 1904.1 cm^{-1} whereas for **2** it appears at 1902.2 cm^{-1} . On the other hand, the shape and the position of the intermediate IR band are the same for precursors **2** and **2D₄** (Figure 5B,C). The frequency of the structured IR band suggests that intermediates with Ga–H bonds are causing these resonances. Interestingly, the fragmentation of **2D₄** does not result in broad and structured IR bands that are shifted to the typical Ga–D stretching region. The broadness of the IR bands indicate that the corresponding molecules are relatively large

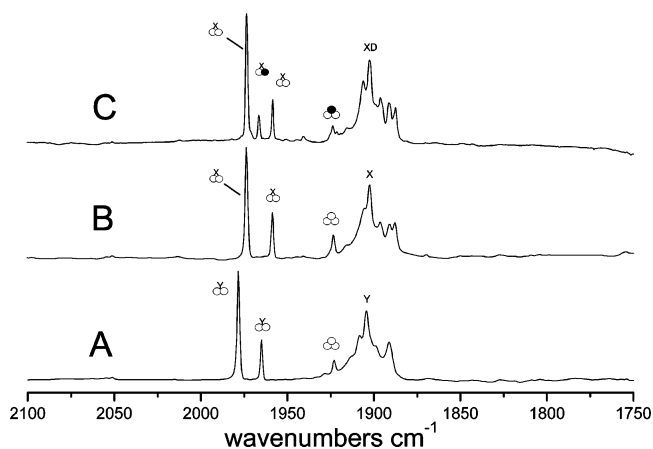


Figure 5. Formation of intermediates at thermolysis temperatures of 750 °C (thermolysis products trapped in an excess of argon at 15 K; y-axis in arbitrary units; see Experimental Section for details). Spectrum A shows matrix-isolated products of a thermolysis of **1**: $\text{O}\times\text{O}$, ClGaH_2 ; OOO , GaH_3 ; Y, $\text{Me}_2\text{N}(\text{CH}_2)_3\text{GaClH}$. Spectrum B shows matrix-isolated products of a thermolysis of **2**: $\text{O}\times\text{O}$, BrGaH_2 ; OOO , GaH_3 ; X, $\text{Me}_2\text{N}(\text{CH}_2)_3\text{GaBrH}$. Spectrum C shows matrix-isolated products of a thermolysis of **2D₄**: $\text{O}\times\text{O}$, BrGaH_2 ; $\text{O}\times\bullet$, BrGaDH ; $\bullet\bullet\bullet$, GaDH_2 ; XD, $\text{Me}_2\text{NCH}_2\text{CD}_2\text{CH}_2\text{GaBrH}$.

in comparison with hydrides such as XGaH_2 ($\text{X} = \text{Cl}, \text{Br}$). Furthermore, the intermediate IR bands appear at lower frequencies compared with those of the Ga–H stretches of X_2GaH and XGaH_2 ($\text{X} = \text{Cl}, \text{Br}$), a fact that can be interpreted as being due to a higher coordination number of the gallium atom for these intermediates.

All these experimental results can be explained if we assume an intermediate gallium hydride that is equipped with only one chelating ligand; i.e., $\text{Me}_2\text{N}(\text{CH}_2)_3\text{GaXH}$ in the case of **1** ($\text{X} = \text{Cl}$) and **2** ($\text{X} = \text{Br}$) and $\text{Me}_2\text{NCH}_2\text{CD}_2\text{CH}_2\text{GaBrH}$ in the case of **2D₄**. On the basis of this hypothesis, we performed HF and B3LYP calculations using 6-31G(d) and 6-311G(d,p) basis sets for the proposed intermediates (Figure 6). We could optimize only two geometries that differ from each other in the position of the envelope tip of the five-membered ring with respect to the substituents H and X (Figure 6). This is illustrated in Figure 6, where two different perspectives are shown for the bromide $\text{Me}_2\text{N}(\text{CH}_2)_3\text{GaBrH}$. Isomer **A** exhibits C3 as the envelope tip, whereas isomer **B** exhibits C2 as the envelope tip. The view along the Ga–N donor bond reveals that for **A** the Ga–H bond is staggered with respect to the NMe_2 moiety; for **B** the GaClH moiety shows an eclipsed arrangement with respect to NMe_2 . In principle, a compound with saturated five-membered ring in an envelope conformation with one chiral center could result in 10 enantiomeric pairs (C_1 point group symmetries). Several attempts have been undertaken to find more than the two isomers depicted in Figure 6, but all optimizations resulted either in **A** or **B**. For example, if the positions of the H and X atoms in isomer **A** were exchanged to get a starting geometry, the optimization resulted in one enantiomer of isomer **B**; a similar procedure starting with **B** resulted in isomer **A**. As expected, the calculation shows that the most intense IR bands are caused by Ga–H stretching modes. Table 3 compiles the Ga–H harmonic frequencies, the intensities, and the relative energies of the two isomers at three levels of theory.

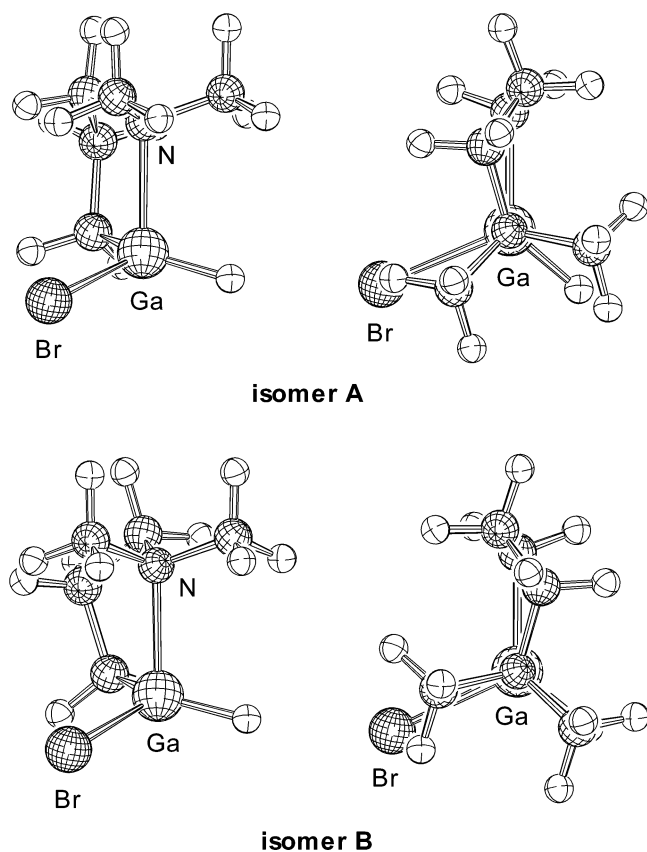
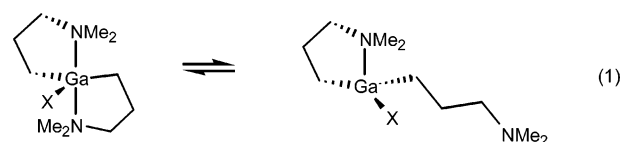


Figure 6. Calculated equilibrium geometries of proposed intermediates $\text{Me}_2\text{N}(\text{CH}_2)_3\text{GaXH}$. Depicted are the bromides at the B3LYP/6-311G(d,p) level of theory. Each isomer is shown from two different perspectives (Keller, E. *SCHAKAL 99, A Computer Program for the Graphical Representation of Molecular and Crystallographic Models*; University of Freiburg: Freiburg, Germany, 2001).

Both isomers have a similar absolute energy with **A** being slightly preferred over **B** at all applied levels of theory (Table 3). If one assigns calculated harmonic Ga–H stretching frequencies for isomer **A** and **B** to the measured IR bands at 1904.1 and 1902.2 for **1** and **2**, respectively, reasonable obsd/calcd frequency ratios are obtained; e.g., compound **1** results in ratios of 0.9422 [HF/6-31G(d)], 0.9614 [B3LYP/6-31G(d)], and 0.9670 [B3LYP/6-311G(d,p)] for isomer **A**. At all applied levels of theory, the predicted frequencies of the chlorides are always a few wavenumbers higher than the ones of the bromides. These differences are 4.7 cm^{-1} (isomer **A**) and 2.7 cm^{-1} (isomer **B**) at the HF level and $5.3/3.1\text{ cm}^{-1}$ (isomer **A**) and $12.0/10.4\text{ cm}^{-1}$ (isomer **B**) at the two B3LYP levels. These differences are not in perfect agreement with the experimental determined difference of 2 cm^{-1} but do not contradict the experiment either (Figure 6). The unequivocal identification of a complex molecule like the proposed intermediate $\text{Me}_2\text{N}(\text{CH}_2)_3\text{GaXH}$ by just one type of vibrational mode is impossible. Therefore, we tried to find other IR bands that belong to the set of resonances around 1900 cm^{-1} . In the temperature range $600\text{--}800\text{ }^\circ\text{C}$, the fragmentation of the precursor is incomplete, and between 600 and $700\text{ }^\circ\text{C}$ the most intense IR bands are caused by undecomposed precursor **1**, **2**, and **2D₄**, respectively. This makes the assignment of further IR bands to the proposed intermediate very difficult. In cases such as this, often it is possible to

eliminate the signals of a remaining starting compound electronically. For alanes and gallanes of the type $\text{Me}_2\text{N}(\text{CH}_2)_3\text{MX}_2$, this procedure helped to identify intermediates, but for any of the three starting gallanes described in this paper an electronic elimination was not successful. It seems that the IR spectra of the nonfragmented precursors are dependent on oven temperatures. That means that a subtraction of a remaining starting compound from a particular spectrum of a thermolysis is not applicable, because an IR spectrum of this precursor without any thermolysis products at these specific thermolysis conditions is unknown. This can be rationalized if we assume that one donor group is lifted off from the gallium atom to give a tetracoordinated species (eq 1). This equilibrium will shift to the right side with increasing temperatures. In addition to the proposed equilibrium, one needs to take into account that the starting precursors with the pentacoordinated gallium atom can exist in different isomers that are distinguished by the position of the envelope tip of the five-membered rings. Furthermore, one expects many isomers for the tetracoordinated species of eq 1 caused by different conformations for the five-membered ring and the open propyl arm.



Conclusions

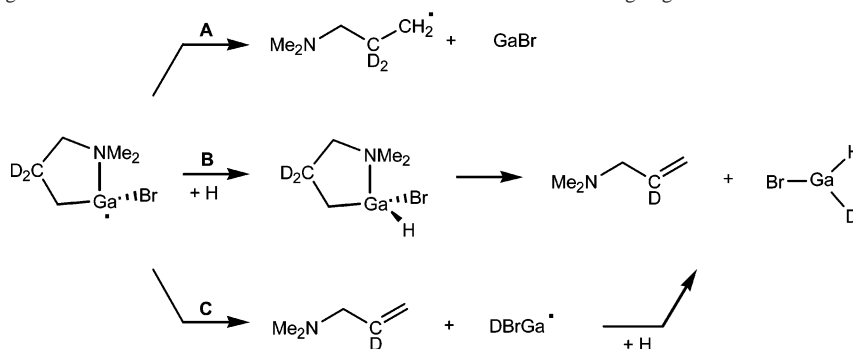
We have identified products of thermolysis reactions of the intramolecularly coordinated precursors **1**, **2**, and **2D₄**. How are these products formed? Matrix-isolation technique allows the reaction products to be identified, but not the complete decomposition mechanisms, which must therefore remain speculative. A matrix-isolation pyrolysis investigation aims at getting snapshots of gaseous reaction products. One intends to identify intermediates that are fragments of an investigated precursor. However, a major difficulty is due to the fact that it is impossible to suppress further reactions of intermediates. These “secondary” reactions can occur in the gas phase and in the evolving matrix. All IR spectra of thermolysis experiments show many IR absorptions, and we have no doubt that the matrices contain other products than those identified so far. All intense IR bands have been assigned to reaction products, and we assume that these are the main products. Furthermore, comparison between the nondeuterated precursor **2** and its deuterated counterpart **2D₄** gives important insights into the decomposition of the organic ligands.

In principle, one expects two major fragmentation pathways for the loss of the chelating ligand: homolysis of a Ga–C bond and β -hydrogen elimination. If β -hydrogen elimination were occurring exclusively, then allyldimethylamine and XGaH_2 would be the only products. In particular, **2D₄** would have resulted in BrGaD_2 , which is obviously not the case. Therefore, we conclude that for a single precursor molecule, both ligands are not detached via β -hydrogen

Table 3. Calculated Harmonic Ga–H Stretching Frequencies [cm^{-1}], Intensities (in Parentheses in km/mol), and Relative Energies (in Brackets in kJ/mol)^a for Isomers **A** and **B** of $\text{Me}_2\text{N}(\text{CH}_2)_3\text{GaXH}^b$

	X = Cl			X = Br		
	HF/6-31G(d)	B3LYP/6-31G(d)	B3LYP/6-311G(d,p)	HF/6-31G(d)	B3LYP/6-31G(d)	B3LYP/6-311G(d,p)
isomer A ^b	2020.9 (242.6) [0.00]	1980.5 (203.0) [0.00]	1969.1 (215.4) [0.00]	2016.2 (246.2) [0.00]	1975.2 (205.1) [0.00]	1966.0 (213.3) [0.00]
isomer B ^b	2022.7 (247.7) [1.82]	1984.0 (206.3) [2.17]	1967.7 (217.6) [1.91]	2020.0 (251.2) [1.48]	1972.0 (208.4) [1.77]	1957.3 (215.4) [1.79]

^a Without inclusion of ZPVE. ^b See Figure 6.

Scheme 1. Proposed Fragmentation Paths for Precursor **2D₄** after the Loss of the First Chelating Ligand


eliminations. On the other hand, this means that homolysis of Ga–C bonds occurs. The indications that this is the case are as follows. For the nondeuterated precursors, we detected $\text{H}_2\text{C}=\text{CH}_2$, $\text{H}_2\text{C}=\text{NMe}$, CH_4 , and HCN ; the deuterated precursor **2D₄** resulted in the same species except for ethylene for which $\text{D}_2\text{C}=\text{CH}_2$ instead of $\text{H}_2\text{C}=\text{CH}_2$ was formed. The experimental fact that $\text{D}_2\text{C}=\text{CH}_2$ has been found as the only isotopomer of ethylene implies that this fragment originates from the chelating ligand $\text{CH}_2\text{CD}_2\text{CH}_2\text{NMe}_2$. These findings are in accordance with the proposed eq 2, where a dimethylaminopropyl radical eliminates ethylene to give a new radical $\text{Me}_2\text{NCH}_2^\bullet$. This radical might eliminate Me^\bullet to give the detected species $\text{H}_2\text{C}=\text{NMe}$, and further decompositions could result in HCN .



This raises the question: is β -hydrogen elimination involved at all in the decomposition process? In the temperature range 700–850 °C, we have identified $\text{H}_2\text{C}=\text{CDCH}_2\text{NMe}_2$ among other reaction products. Additional support for the formation of allyldimethylamine comes from the detection of allyl radicals. Compound **2** resulted in $[\text{H}_2\text{CCHCH}_2]^\bullet$ whereas **2D₄** selectively gave $[\text{H}_2\text{CCDCH}_2]^\bullet$. First of all, this suggests that this C_3 fragment originates from the propyl group of the chelating ligand. Interestingly, at thermolysis temperatures of 700 °C the signals of $\text{H}_2\text{C}=\text{CDCH}_2\text{NMe}_2$ are clearly visible, but the two strongest IR absorptions of $[\text{H}_2\text{CCDCH}_2]^\bullet$ at 803.0 and 786.6 cm^{-1} are just distinguishable from the background. This situation changes with increasing temperature. From 700 to 750 to 800 °C we measured a small increase in intensities for both products, but from 800 to 850 °C the intensity of the 922.8/919.7 “doublet” ($\text{H}_2\text{C}=\text{CDCH}_2\text{NMe}_2$) decreased whereas the in-

tensity of the IR bands at 803.0 and 786.6 cm^{-1} strongly increased. At temperatures of 900 and 1000 °C allyldimethylamine was no longer detectable but $[\text{H}_2\text{CCDCH}_2]^\bullet$ still resulted in intense signals. We interpreted this behavior as an indication that allyldimethylamine is produced by the thermolysis process and is further decomposed to give allyl radicals and $\text{Me}_2\text{N}^\bullet$ (eq 3). The latter radical presumably is a source for H^\bullet , HCN , Me^\bullet , and $\text{H}_2\text{C}=\text{NCH}_3$. This interpretation is supported by the known method to produce allyl radicals by gas-phase pyrolysis of allyl halides.³⁴



The occurrence of allyldimethylamine suggests that β -hydrogen elimination is involved in the thermolysis process. This interpretation is based on our experience with alanes and gallanes of the type $\text{Me}_2\text{N}(\text{CH}_2)_3\text{MX}_2$ ($\text{M} = \text{Al}$ and $\text{X} = \text{Cl}, \text{Br}$;^{43,44} $\text{M} = \text{Ga}$ and $\text{X} = \text{Cl}, \text{Br}, \text{N}_3, \text{Me}$)^{16,19} where we have shown that only the dimethylgallane fragments via a β -hydrogen elimination route. Only in this particular case were we able to identify allyldimethylamine among the reaction products. In all other cases, the chelating ligand was eliminated through radical processes; e.g., the selectively deuterated species $\text{Me}_2\text{NCH}_2\text{CD}_2\text{CH}_2\text{MBr}_2$ fragmented to give monomeric HMBR_2 and not DMBr_2 .⁴⁴

The precursor compounds **1**, **2**, and **2D₄** eliminate their chelating ligands one after the other. This is suggested by the detection of intermediate gallium hydrides $\text{Me}_2\text{N}(\text{CH}_2)_3\text{GaXH}$ and $\text{Me}_2\text{NCH}_2\text{CD}_2\text{CH}_2\text{GaBrH}$, respectively (Figures 5 and 6). IR bands of respective deuterides could not be detected. These results can be rationalized if one assumes that the first donor ligand is eliminated by a homolysis of a

(43) Müller, J.; Wittig, B. *Eur. J. Inorg. Chem.* **1998**, 1807–1810.

(44) Müller, J.; Wittig, B. *Proc.—Electrochem. Soc.* **2001**, 13, 124–128.

Ga–C bond (depicted for precursor **2D₄** in Scheme 1). The resulting gallium radical $[\text{Me}_2\text{NCH}_2\text{CD}_2\text{CH}_2\text{GaBr}]^\bullet$ might further react in three different ways (Scheme 1).

First, route A shows a decomposition to GaBr and another equivalent of a dimethylaminopropyl radical discussed before. Second, the gallium radical could trap an H atom (route B) to give the hydride $\text{Me}_2\text{NCH}_2\text{CD}_2\text{CH}_2\text{GaBrH}$. This interpretation is consistent with our results obtained with precursors of the type $\text{Me}_2\text{N}(\text{CH}_2)_3\text{MX}_2$, which resulted in monomeric hydrides even though β -hydrogen elimination was not involved.^{15,18,43,44} These results clearly show a principle difficulty within matrix-isolation pyrolysis investigations. Instead of an intermediate radical, a hydrogen saturated “secondary” product was identified in matrix. Third, route C illustrates the possibility that first β -hydrogen elimination occurs to give allyldimethylamine and GaBrD^\bullet followed by a saturation reaction with H atoms. Via route B and C, the presence of BrGaDH and $\text{H}_2\text{C}=\text{CDCH}_2\text{NMe}_2$ can be explained. However, precursor **2** would result in BrGaH_2 via route B and C, but this dihydride is the main product in the experiments with **2D₄**, too. Therefore, route B and C cannot be the main path to BrGaH_2 , and the question remains how this dihydride is formed. The known compound ClGaH_2 was synthesized in Ar matrices by co-condensation reactions of GaCl with H_2 .²⁶ Gallium(I) chloride was introduced into the vacuum system by passing Cl_2 over liquid Ga at 1170 K. Finally, irradiation with an Hg high-pressure lamp gave ClGaH_2 .²⁶ Recently, the mechanism of the reaction of H_2 with MCl ($\text{M} = \text{Ga}, \text{In}$) was investigated with theoretical methods.⁴⁵ This work confirmed that the molecules MCl and H_2 do not react spontaneously. However, a spontaneous formation of monomeric gallium hydrides had been obtained in matrix-isolation experiments from thermally produced metal atoms co-condensed with H atoms.²⁵ On the basis of these results, one can speculate that the dihydrides XGaH_2 ($\text{X} = \text{Cl}, \text{Br}$) are formed from GaX and H atoms, with the latter being produced from the radical fragmentation pathways of the chelating ligand (Scheme 1; eqs 2 and 3). A formation of XGaH_2 from GaX and H atoms would proceed through intermediates XGaH^\bullet , and consequently, we tried to identify these unknown radicals. According to B3LYP calculations, the Ga–H stretching modes are expected at 1675.5 cm^{-1} and at 1676.0 cm^{-1} with intensities of 130 and 136 km/mol for ClGaH^\bullet and BrGaH^\bullet , respectively (see Experimental Section for details). However, we could not find IR bands in the expected region that could be assigned to XGaH^\bullet . Of course, this does not mean that these radicals are not trapped in matrices; they might be present in small amounts. Additionally, a formation of BrGaDH from GaBr with H and D atoms is also feasible.

It seems likely that the presence of hydrogen atoms is the cause for the formation of GaH_3 . This species had been

identified for the first time in 1994 from co-deposition reactions of Ga and H atoms.²⁵ It is quite possible that GaH_3 , which was observed in the thermolysis of precursor **1** and **2**, results from reactions of Ga and H atoms. The formation of Ga atoms in a CVD process using the diazido precursor $\text{Me}_2\text{N}(\text{CH}_2)_3\text{Ga}(\text{N}_3)_2$ were monitored with REMPI mass spectrometry.⁴⁶ Therefore, we assume that a fragmentation of compounds **1**, **2**, and **2D₄** also produces Ga atoms. Interestingly, precursor **2** results in GaH_3 and GaH whereas **2D₄** results in GaH_3 , GaDH_2 , GaH , and GaD . Among the gallium(III) species, GaDH_2 is the main compound. Among the gallium(I) species, GaD is the prominent compound with the GaD/GaH ratio being strongly dependent on applied thermolysis temperatures. To date, we cannot explain these experimental facts. However, if the hydrides and deuterides exclusively result from reactions of H, Ga, and D atoms in the evolving matrices, then one would expect a strong dominance of gallium hydrides, because H atoms diffuse faster than D atoms and the concentration of H atoms is expected to be much higher than the one of D atoms (H to D ratio in **2D₄** is 5 to 1).

In summary, we have shown that the intramolecularly coordinated gallium chlorides and bromides, chemically rather simple compounds, exhibit a complex fragmentation behavior. Involved in the loss of the organic ligands are Ga–C homolysis as well as β -hydrogen elimination. Among the thermolysis products, we have identified the monomeric gallanes BrGaH_2 and BrGaDH for the first time. The precursors investigated within this study serve as model compounds for the azides of the type $[\text{Me}_2\text{N}(\text{CH}_2)_3]_2\text{MN}_3$ ($\text{M} = \text{Al},^{10,47} \text{Ga},^{12} \text{In}^{13,47-49}$), which had been used for the group 13 nitride deposition (MOCVD). Recently, we have started to investigate the fragmentation process of these azido species with the intent of a deeper understanding of the MOCVD process. We hope to report on the results shortly.

Acknowledgment. This work was supported by the Fonds der Chemischen Industrie, by the Deutsche Forschungsgemeinschaft, and by a Discovery Grant of the Natural Sciences and Engineering Research Council of Canada.

Supporting Information Available: Calculated bond lengths and angles for H_2GaX ($\text{X} = \text{Cl}, \text{Br}$) at B3LYP/6-311+G(2d,p) and MP2(fc)/6-311+G(2d,p), and Cartesian coordinates for all calculated structures. This material is available free of charge via the Internet at <http://pubs.acs.org>.

IC035496A

(46) Schäfer, J.; Wolfrum, J.; Fischer, R. A.; Sussek, H. *Chem. Phys. Lett.* **1999**, *300*, 152–156.

(47) Fischer, R. A.; Miehr, A.; Ambacher, O.; Metzger, T.; Born, E. *J. Cryst. Growth* **1997**, *170*, 139–143.

(48) Fischer, R. A.; Sussek, H.; Miehr, A.; Pritzkow, H.; Herdtweck, E. *J. Organomet. Chem.* **1997**, *548*, 73–82.

(49) Devi, A.; Parala, H.; Rogge, W.; Wohlfart, A.; Birkner, A.; Fischer, R. A. *J. Phys. IV* **2001**, *11*, 577–584.

(45) Himmel, H.-J. *J. Chem. Soc., Dalton Trans.* **2002**, 2678–2682.